Oil Beneath Arctic Ice: Predicting Under-Ice Storage Capacity as a Means to Better Anticipate Oil Slick Spreading Under Ice

K. Frazier, B.A.
University of Alaska, Anchorage, Alaska, United States of America

T. Ravens, Ph.D.
University of Alaska, Anchorage, Alaska, United States of America

ABSTRACT: In the event of an Arctic oil spill, ice in the water is a complicating factor. The presence of ice complicates the forecasting of the movement and spreading of oil as well as the planning of the oil spill clean-up process. The underside of Arctic sea ice is not flat, rather it presents non-geometric, unpredictable protrusions into the water column. The depth to which these protrusions grow relates to the longevity of the ice itself. The challenge faced by the oil spill forecaster is that information on the under-ice storage capacity is not readily available. Hence, we explored how to estimate under-ice storage capacity based on the ice stage.

Historical reports on Arctic sea ice stage (e.g., first year, thin ice) were obtained from the Alaska Ocean Observing System. Ice stage data is available daily in the form of an ice "egg" code, similar to the CIS/WMO egg. Next, we acquired historic data on under-ice storage capacity. During the winters of 2010-2013, Shell deployed upward looking sonar at several sites in the Beaufort and Chukchi Seas. The sonar made direct measurements of ice draft. The under-ice storage capacity - defined as the volume of pore space above the average ice draft level – was estimated based on the ice draft data.

Analyzing the ice draft alongside the ice stage data, we developed low, medium, and high estimates of oil storage capacity. When the primary ice stage is assigned an ice egg code of 1 to 3, storage capacity is deemed 'low,' identified by less than 15,000 m3/km2. For primary ice stage with a 7 to 10 ice egg code, storage capacity is 'medium,' between 15,000 and 50,000 m3/km2. Older ice with an ice egg code of 11 or greater has a 'high' storage capacity of 50,000 to 80,000 m3/km2.

KEY WORDS: Ice draft, Ice egg, Oil spill, Storage capacity.

1 INTRODUCTION

The National Oceanic and Atmospheric Administration (NOAA) operates an oil spill model referred to as the General NOAA Operational Modeling Environment (GNOME). Until relatively recently, GNOME did not account for the influence of sea ice and its influence on oil slick spreading (Zelenke et al. 2012). However, the recent interest in Arctic oil exploration has made the development of an Arctic-capable GNOME model imperative.

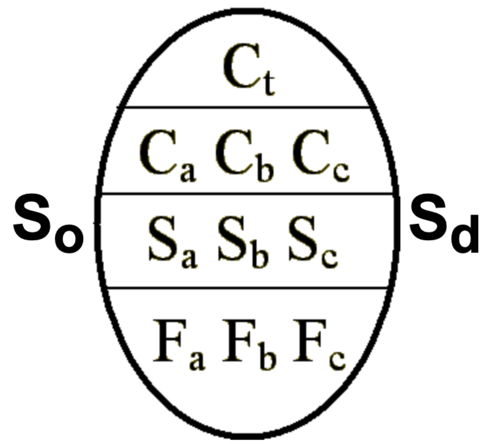

Figure 1. Example ice “egg code” as reported by AOOS concerning Arctic ice conditions.

The goal of this project was to develop an estimate of the under-ice storage capacity of sea ice based on real time data. Real time data allows an oil spill model to update quickly and efficiently during times of crisis. One consistent and reliable source for ice data comes from the U.S. National Ice Center (NIC). There, multiple data sets from the POES and GOES satellites are interpreted and a daily report is produced regarding ice conditions and concentrations for all US waters in the arctic. This report communicates ice conditions in different arctic regions through an ice “egg code,” like that in Figure 1.

The egg code, named for its unique reporting shape, offers a convenient coding scheme which was developed by the World Meteorological Organization (WMO, 1970). This scheme reports the total concentration of ice cover (C_t) at the top of the egg for a given area. Moving down the egg, the second line lists the partial concentrations ($C_{a,b,c}$) of ice in order of decreasing thicknesses, the third line lists the stages of development of the ice ($S_{a,b,c}$), and the bottom of the egg lists the predominant form of the ice, or ice floe size ($F_{a,b,c}$). The remaining development stages, or the age of the remaining ice types, are reported on the outside of the egg, noted as S_o for trace amounts of ice, and S_d for thinner ice. These extraneous categories are used when there is an unusual ice presence or composition in the area. Egg codes for this study were obtained through the Arctic Ocean Observing System (AOOS) and it was noted that some of the historic data differed from convention, as numerous samples did not provide stage (line 3) in order of decreasing thickness. The egg code provided the foundation from which a relationship between the surface and subsurface might be developed. To achieve an under-ice storage capacity estimation, we investigated how well the observed ice condition reports correlated with the measured under-ice storage capacity.

Sea ice is characterized by sub-surface roughness. This roughness ranges from slight impressions to large cavities formed between drafts (Wadhams et al. 2006, Rothrock and Thorndike 1980). Multi-year ice tends to have greater roughness than first year ice (Comfort and Purves 1982, Kovacs 1977). The roughness of the sub surface of sea ice

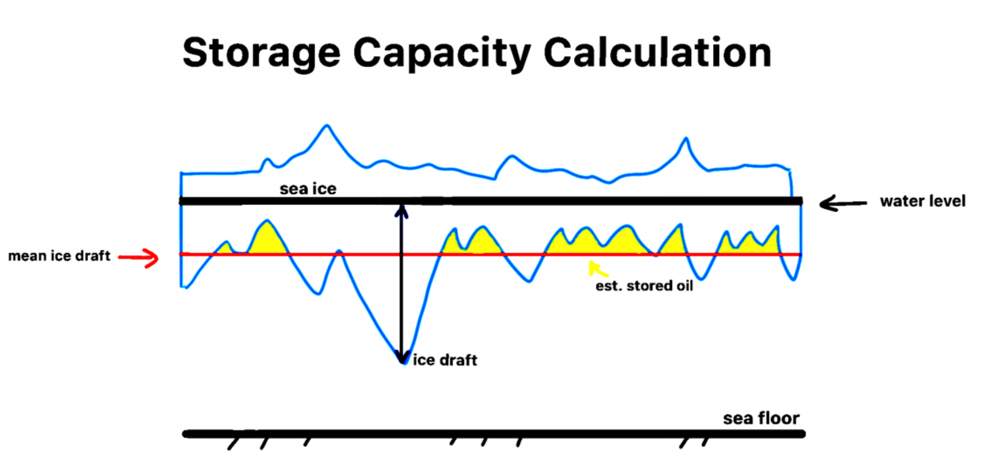

Figure 2. Schematic of the underside of sea ice showing the theoretical under-ice storage capacity.

influences how an oil slick will spread in ice covered water. Oil, being buoyant, will fill the cavities in the underside of the ice (Venkatesh et al 1990). Glaeser and Vance (1971) studied this phenomenon using several small-scale releases of crude oil beneath pack ice in the Chukchi Sea. They noted that oil under the ice did not spread if sufficient storage space was available in the void spaces. When the storage space was filled, the oil spilled over into adjacent spaces. While buoyant, viscous, and surface tension forces also play a role in subsurface spreading, Fingas and Hollbone (2003) and Afenyo et al. (2016) describe under ice topography as one of the dominant factors in determining slick spread. Hence, in order to be able to predict the spreading of oil under ice, it is important to quantify the under-ice storage capacity based on under-ice topography.

2 MEASUREMENT PRINCIPLES

While under-ice storage capacity is a known influence in arctic oil spill modeling, there is some question in the literature as to how to define a storage variable. There was effort by Puskas et al. (1987) to quantify roughness in their equations for determining oil slick thickness. They associated storage capacity with hydraulic roughness, but this roughness acted more as a correction factor and was assumed to be constant. In reality, Arctic sea ice void space grows and wanes during the winter season. As those spaces change, the storage capacity also needs to change. A better descriptor is the relationship developed by LeSchack and Chang (1977) relating the RMS ice draft to potential storage capacity (Equation 1). For our purposes, we followed this definition for the under-ice storage capacity as the pore space above the time average ice draft level (Figure 2).

$$\delta_{sc} = \frac{\iint((h'_{ice} > h_{mean}) - h_{mean})dxdy}{A_d} \qquad [1]$$

Where, δ_{sc} = Storage capacity of the ice (m^3/km^2), h_{mean} = Mean ice draft over a given length (m), h_{ice}' = Ice draft at a position at (x,y) (m), and A_d = Domain area of ice surface (km^2).

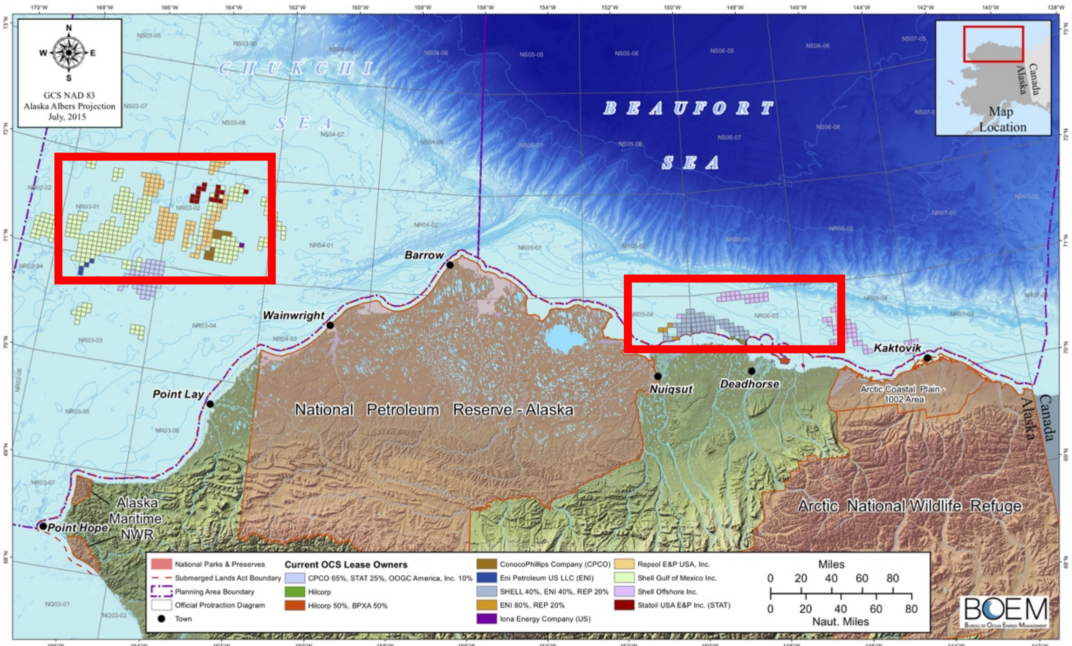

Figure 3. General locations (in red) of Shell and ASL data collection sites, 2005-2013 (BOEM 2015).

3 METHOD

3.1 Data

This project utilized ice draft data published by the North Slope Science Initiative (NSSI), who obtained the information from Shell Exploration and Production Company (Shell). Shell contracted with ASL Environmental Sciences Inc. (ASL) to collect the sub-surface ice draft data in the Beaufort and Chukchi Seas (Figure 3). Data collection began in the Beaufort Sea in 2005, and shifted to the Chukchi Sea in 2008. In the Beaufort, five different locations were used over a period of five years. In the Chukchi, measurements varied among four locations over an eight year time frame. For these programs, two tandem sensors were deployed consisting of an ASL Ice Profiling Sonar (IPS-5), manufactured by ASL, and the Teledyne RD Instruments Acoustic Doppler Current Profiler (ADCP) (Figure 4). These instruments made direct measurements of ice draft, ice velocity, and ocean current profiles. The time resolution on the draft measurement was once every 1-to-2 seconds, with a horizontal resolution of 1 m, and a vertical resolution of 0.025 m. Ice velocity and ocean current profiles from the ADCP were recorded with a time resolution of once every fifteen minutes in 2008-2009 and reduced to once every five minutes from 2009 to 2014 (Mudge et al 2014).

Profiler pairs were moored in water 20-40 m deep and took continuous recordings for up to a year at a time. Each instrument set was recovered annually to replace batteries, perform regional calibrations, and allow download of the data. Timing checks were performed on the instrumentation to measure clock drift. Once checks were complete, the profilers were immediately redeployed to their same mooring site. This study utilized data sets collected between 2010 and 2013 and from two mooring locations: one in the Beaufort ('Site A') and one in the Chukchi Sea ('Crackerjack') (Mudge et al 2014).

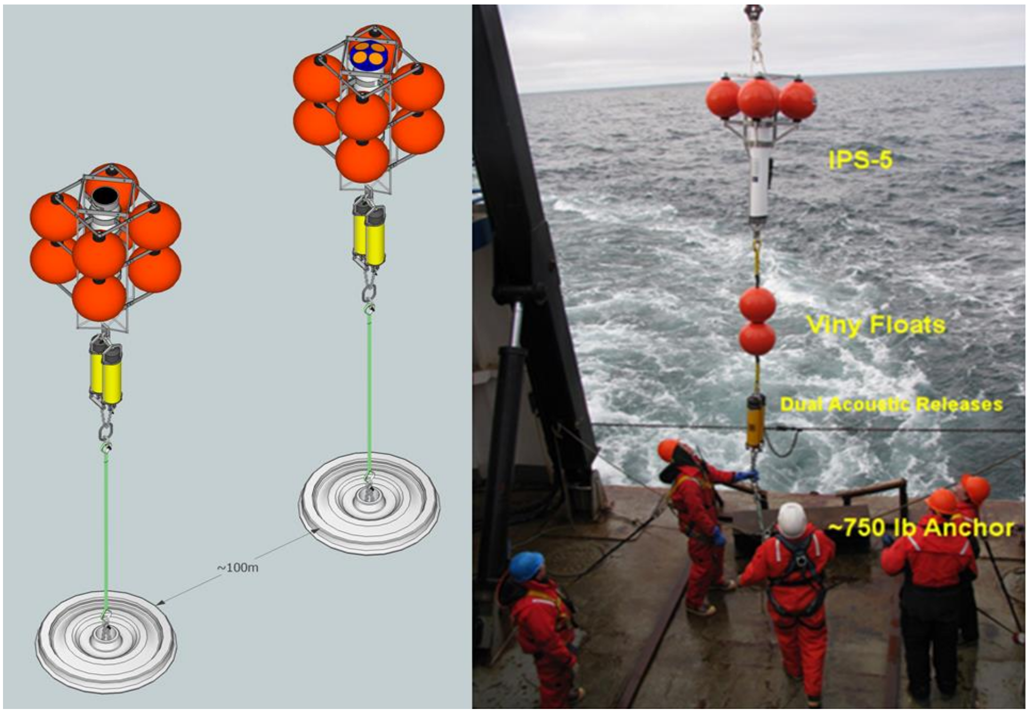

Figure 4. Schematic diagram of the taut line moorings used for deployment of the IPS (left) and ADCP (right) instruments (Mudge et al. 2014).

Table 1. Ice "egg code" used to define ice stage.

Ice Egg Code	1	2	3	4	5	6	7
Modified Code	1	2	3	4	5	6	7
Thickness (cm)	0-10	10-30.	10-15.	15-30.	15-30.	30-200.	30-70.
Description:	New, Frazil, Slush, etc	Nilas, Ice Rind	Young	Gray	Gray - White	1Y	1Y, Thin
Ice Egg Code	8	9	1*	4*	7*	8*	9*
Modified Code	8	9	10	11	12	13	14
Thickness (cm)	30-70.	30-70.	70-120.	>120	>2m	>2m	>2m
Description:	1Y, Thin, Stage 1	1Y, Thin, Stage 2	1Y Ice, Medium	1Y Ice, Thick	Old 1Y Ice	SY Ice	MY Ice

3.2 Code

The raw ice draft data was processed by ASL and followed established procedures documented by Melling et al. (1995), Fissel et al. (2008) and ASL Environmental Sciences Inc. (2011). This procedure converted the time-of-travel recorded data into a spatial data series using the recorded ice velocities. Processed data was then imported and analyzed using Matlab to compute a weekly mean draft, the subsurface cavity width between drafts, and number of cavities in the measured domain. Quality control of the data is also built-in and the Matlab function eliminates ice data where drafts appear to hover or revisit in the same area. Subsurface storage capacity is the total computed volume over a measured area and is reported in units of m3/km2.

3.3 Surface Conditions

The ice stage above each ADCP/IPS data point during the 2010-2013 measurement period was obtained from AOOS. Ice stage data is available in the form of the ice egg code (described above) and is available on a weekly basis. The code (Table 1) includes fourteen ice stage designations. This project converted ice stage at a given location and time into a single, comma separated identifier, such as '1,3,7' or '10,11,12'. This project modified the reported WMO standard egg code so that final data could be sorted in Excel. The relationship between the standard code and the modified code is listed in Table 1.

4 RESULTS

Weekly subsurface storage capacity estimations, in combination with the associated surface condition ice egg condition, are graphed in Figure 5. When sorted by increasing stage of the thickest fraction of the ice, a distinct trend in the data becomes apparent. Generally, as the ice ages, storage capacity increases. There does appear to be a maximum capacity which develops, after which, subsurface storage capacity declines. Fast ice, or ice that is connected to the land, generally develops later in the season but its relative storage capacity is low. This type of ice may experience subsurface smoothing by the current due to its stationary nature.

Weekly estimations that significantly over or under estimated storage capacity or didn't pass the quality control algorithm were excluded from the final results. Over the three-year sample period, 183 capacity calculations were considered valid from which to draw a relationship. Excluded data included sets that produced a large storage capacity in relatively new or melting ice, which occurs when the battery in the IPS gets weak and the system malfunctions. Ice draft measurements that were taken under ice that appeared to hover over the same area was also excluded. These measurements would have erroneously skewed the storage capacity estimation when converted to a spatial data series. Additionally, the weekly periods for which ice draft was calculated, and surface conditions were reported, did not always align, often separated by two or three days.

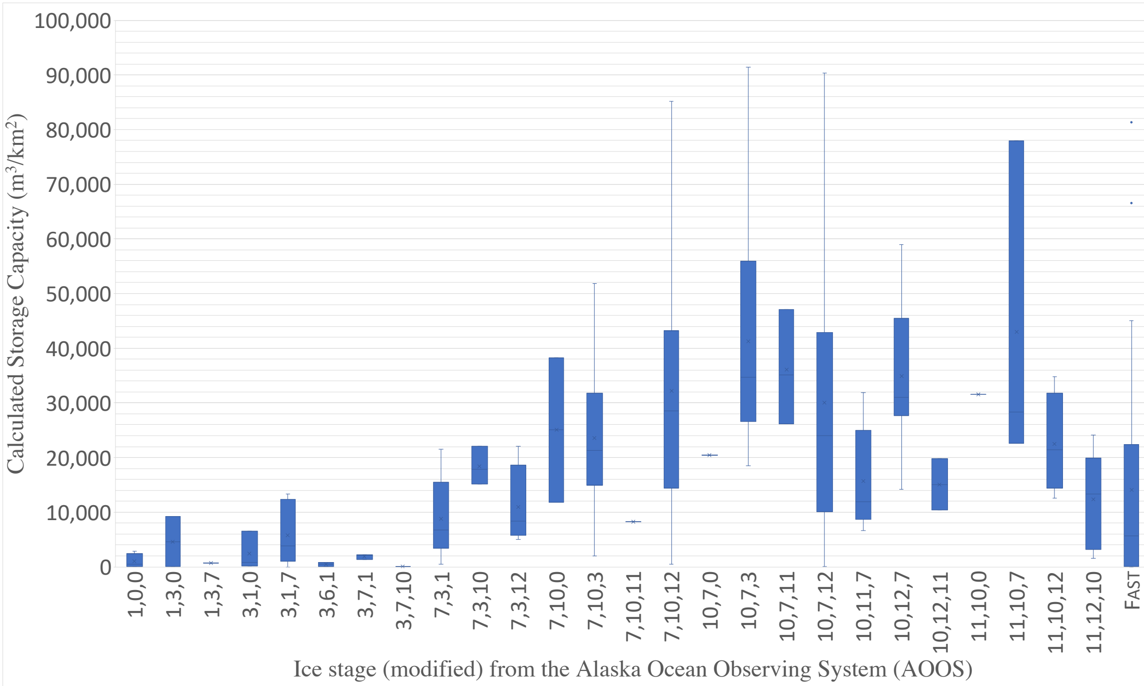

Figure 5. Sea ice sub-surface storage capacity compared to observed ice surface stage.

From the graphical analysis, oil storage capacity beneath sea ice can now be estimated on a low, medium, and high spectrum, which appears to be positively correlated to the stage of the thick ice fraction present. When the ice stage of the thickest ice fraction is assigned an ice egg code of 1 or 3 (Table 1), storage capacity is 'low,' identified by less than 15,000 m^3/km^2 of void space. For a primary ice stage with a 7 or 10, storage capacity is 'medium,' between 15,000 and 50,000 m3/km2. Older ice with an ice egg code of 11 or greater has a 'high' storage capacity of 50,000 to 80,000 m^3/km^2.

5 DISCUSSION

This project is intended to be a first step in quantifying subsurface storage capacity and is by no means complete. After computing the average draft, storage capacity was linearly extrapolated over the region. While this offers a satisfactory estimation, it does not adequately characterize the underside of the sea ice. Utilizing multi-beam sonar data of the underside of sea ice would provide a better picture of the relative roughness of the ice in relation to its observable surface conditions. This estimation may over or under estimate the actual void space and needs to be further investigated.

Another area of development is the definition of storage capacity. Defining capacity as the space between the ice surface and the time average draft may improperly quantify the actual space available. During peak growth and melt seasons, the stage of the ice is rapidly changing. Brine channels in the ice may provide additional storage that is not yet accounted for. Also, a week may be too long over which to average the draft data. The depth of the average draft may also lead to improper estimations of storage capacity. Further research into how to define the lower threshold above which volume is computed is recommended.

Finally, there is some question as to what future subsurface storage capacity estimations will look like. The effects of global climate change in the Arctic are seen in the decrease in old, multi-year ice and the prevalence of first year ice. Prior to the 1970s, multi-year ice covered more than two thirds of the Arctic Basin (Kwok and Untersteiner, 2011). Over the past 30 years, however, that fractional cover of multi-year ice has significantly decreased. In fact, this work was only able to provide estimations for the storage capacity of ice ranging from frazil to thick, first year ice. No multi-year ice passed over either IPS locations. Future storage capacity calculations may only need to consider ice ranging from new to thin, first year ice.

6 CONCLUSION

The modeling and forecasting of the movement and spreading of oil spilled under ice is challenging. By defining the under-ice storage capacity and by finding ways to estimate storage capacity based on readily available data on ice stage, our project has yielded an important tool for forecasting the spreading of oil spilled under ice. Estimates of the spatial extent of oil spilled under ice will help first responders plan clean-up procedures.

ACKNOWLEDGMENTS

This project was conducted in support of the Arctic Oil Spill Modeling project initiated in 2017 with the Arctic Domain Awareness Center (ADAC), a Center of Excellence for maritime research for the Department of Homeland Security, under Grant Award Number 2014-ST-061-ML0002-03, and in collaboration with the National Oceanic and Atmospheric Administration (NOAA). Research support was provided by faculty at the University of Alaska, Anchorage and Texas A&M University. Thank you to center staff and to our collaborators for their enormous efforts in this endeavor. Also, thank you to Dana Brunswick who, during the course of her thesis, provided invaluable assistance in the importation and utilization of the NSSI data sets.

REFERENCES

ASL Environmental Sciences Inc. (2011). *IPS Processing Toolbox User's Guide. 2011*. Report by ASL Environmental Sciences Inc., Victoria BC Canada.

Afenyo, M., Veitch, B., & Khan, F. (2016). *A state-of-the-art review of fate and transport of oil spills in open and ice-covered water.* Ocean Engineering, 119, 233-248. DOI: 10.1016/j.oceaneng.2015.10.014

Bureau of Ocean and Energy Management (BOEM), *GCS NAD 83 Alaska Albers Projection*. 2015. [cited 25 March 2019]. Available from: https://www.boem.gov/uploadedFiles/BOEM/About_BOEM/BOEM_Regions/Alaska_Region/Leasing_and_Plans/Plans/Map%202.pdf

Comfort, G., & Purves, W. (1982). *Behaviour of Crude Oil Spilled Under Multi-Year Ice*. EPS 4-EC-82-4 August 1982. Environment Canada, Environmental Protection Service, Ottawa, Ontario.

Fingas, M., & Hollebone, B. (2003). *Review of behaviour of oil in freezing environments*. Marine Pollution Bulletin, *47*(9-12), 333-340. DOI: 10.1016/s0025-326x(03)00210-8

Fissel, D.B., Marko, J.R., and Melling, H. (2008.) *Advances in Upward Looking Sonar Technology for Studying the Processes of Change in Arctic Ocean Ice Climate*. Journal of Operational Oceanography, 1(1): 9-18.

Glaeser, J.L., & Vance, G.P. (1971). *A study of the behavior of oil spills in the Arctic*. U.S. Coast Guard, Applied Technology Division. Washington, DC.

Kovacs, A. (1977). *Sea ice thickness profiling and under-ice oil entrapment.* Offshore Technology Conference. DOI: 10.4043/2949-ms

Kwok, R., & Untersteiner, N. (2011). *The thinning of arctic sea ic*e. Physics Today, 64(4), 36-41. doi:10.1063/1.3580491

LeSchack, L.A., and Chang, D.C. (1977). *Arctic under-ice roughness.* Development and Resources Transportation Co. Silver Spring, MD.

Melling, H., P.H. Johnston and D.A. Riedel. (1995). Measurements of the underside topography of sea ice by moored subsea sonar. J. Atmospheric and Oceanic Technology, 13(3): 589-602.

Mudge, T.D., Fissel, D.B., Barrette, J., Sadowy, D., Borg, K., Billenness, D., Wolf, M., Bryce, A., Slonimer, A., Milutinovic, N., Lim, J., Lawrence, J., and Martinez, M. (2014). *Analysis of Ice and Metocean Measurements, Beaufort Sea 2012-2013, for Shell*. Project Report for Shell International Exploration and Production Inc., Houston, Texas by ASL Environmental Sciences Inc., Victoria, B.C. Canada. 14-24.

Puskas, J.K., McBean, E.A., Kouwen, N., 1987. *Behaviour and transport of oil under smooth ice*. Canadian Journal of Civil Engineering 14, 510–518.

Rothrock, D. A., & Thorndike, A. S. (1980). *Geometric properties of the underside of sea ice.* Journal of Geophysical Research: Oceans, 85(C7), 3955-3963.

Venkatesh, S., El-Tahan, H., Comfort, G., & Abdelnour, R. (1990) *Modelling the behaviour of oil spills in ice-infested waters*. Atmosphere-Ocean, 28:3, 303-329, DOI: 10.1080/07055900.1990.9649380

Wadhams, P., Wilkinson, J. P., & McPhail, S. D. (2006). *A new view of the underside of Arctic sea ice*. Geophysical Research Letters, 33(4).

WMO. (1970). *WMO Sea-Ice Nomenclatur*e. Secretariat of the World Meteorological Organization.

Yang, M., Khan, F., Garaniya, V., & Chai, S. (2015). *Multimedia fate modeling of oil spills in ice-infested waters: An exploration of the feasibility of fugacity-based approach.* Process Safety and Environmental Protection, *93*, 206-217. doi: 10.1016/j.psep.2014.04.009

Zelenke, B., C. O'Connor, C. Barker, C.J. Beegle-Krause, and L. Eclipse (Eds.). (2012). *General NOAA Operational Modeling Environment (GNOME) Technical Documentation*. U.S. Dept. of Commerce, NOAA Technical Memorandum NOS OR&R 40. Seattle, WA: Emergency Response Division, NOAA.